

# Submerged hollow fiber ultrafiltration as seawater pretreatment in the logic of integrated membrane desalination systems

Gianluca Di Profio<sup>a,b,\*</sup>, Xiaoshen Ji<sup>b</sup>, Efrem Curcio<sup>b</sup>, Enrico Drioli<sup>a,b,c</sup>

<sup>a</sup> Institute on Membrane Technology (ITM-CNR), Rende, Italy

<sup>b</sup> Department of Chemical and Materials Engineering, University of Calabria, Rende, Italy

<sup>c</sup> Hanyang University, WCU Energy Engineering Department, Seoul, South Korea

## ARTICLE INFO

### Article history:

Received 23 July 2010

Received in revised form 18 October 2010

Accepted 19 October 2010

Available online 10 November 2010

### Keywords:

Hollow fiber membranes

Integrated membrane systems

Seawater desalination

Seawater pretreatment

Submerged ultrafiltration

## ABSTRACT

Integrated membrane systems have been recently proposed as suitable alternatives to overcome existing limitations in traditional seawater reverse osmosis desalination plants. By this approach, submerged hollow fiber ultrafiltration have been chosen as pretreatment because of the lower energetic consumption and the great significance for reducing particles deposition on the membrane. This work focuses on the study of the influence of a set of operating conditions and the fouling dynamics when operating submerged ultrafiltration under subcritical flux conditions for relatively long-time.

According with results, submerged hollow fiber ultrafiltration can be considered as a feasible pretreatment in reducing natural organic matter from seawater, provided that the opportune operating conditions were well identified and optimized.

© 2010 Elsevier B.V. All rights reserved.

## 1. Introduction

In traditional seawater reverse osmosis (SWRO) desalination plants there is the need to overcome existing limitations by increasing water quality, enhancing the overall recovery factor, reducing the environmental impact of brine and its management costs, and extending membrane lifetime, thus making seawater (SW) desalination more affordable economically. Integrated membrane systems (IMs) have been receiving recently increasing consideration as efficient means for the implementation of process intensification strategy and the optimization of productive cycles [1,2]. A possible application of such strategy in SWRO desalination has been put in practice by integrating advanced pre- and posttreatment membrane operations with reverse osmosis (RO), thus realizing systems working on the concepts of (quasi) zero-liquid discharge and total recovery of raw materials [3]. According to this scenario, pressure-driven membrane operations (microfiltration: MF, nanofiltration: NF, and ultrafiltration: UF) are used as pretreatment to RO, while membrane contactors, in the form of membrane crystallization (MCR) and/or membrane distillation (MD), operate on the brines of NF and RO (Fig. 1) [4] (<http://medina.unical.it>). Low-pressure membrane pretreatment will remove suspended solids, particles, turbidity, microorganisms, and some natural organic matter (NOM) from seawater. NF will remove low molecular weight organic substances and the most part of bivalent ions, so that lower fouling

water can be fed directly to RO which, in turns, will operate at lower pressure because of the reduced osmotic pressure, thus increasing membrane lifetime while reducing its energetic duty. In the posttreatment stage the brine produced in the RO and NF units can be converted into valuable products, like pure crystals with the required morphology (size, size distribution, shape, and habit) and structure (polymorphism), by MCR [5]. In such IMS, RO membrane fouling would consistently be reduced, the overall water recovery factor can be increased up to 95%, the costs for chemicals and for brine disposal will consistently be reduced (or eliminated) by producing added-value crystals, and the cost for desalted water can be reduced well below 0.5 US\$/m<sup>3</sup> [6], making seawater desalination economically affordable worldwide. In order to achieve these results, advanced water pretreatment operations are necessary to reduce/remove natural organic substances existing in seawater with the aim: (1) to reduce the amount of those species which might act directly as foulant for the RO membranes or would be nutrients for microorganisms, which generate biofouling, and (2) to avoid their hindrance/influence with the crystallization mechanism, by adsorption over the crystal embryos or by incorporation into the crystal lattice, thus leading to the cessation of growth or to the production of crystals with undesired or uncontrolled properties.

As membrane pretreatment, ultrafiltration is already being used as an efficient technique to get consistent and high quality seawater prior to RO [7–26]. The main advantages of UF compared to the conventional pretreatments are the improved water quality, the small footprint, the small amount of chemicals required and the stable operation [25], while being competitive in terms of the overall costs [13,26]. However, the delicate problem concerning the performances of UF is the serious

\* Corresponding author. Via P. Bucci Cubo 17/C, 87036 Rende (CS), Italy. Tel.: +39 0984 492010; fax: +39 0984 402103.

E-mail address: [g.diprofio@itm.cnr.it](mailto:g.diprofio@itm.cnr.it) (G. Di Profio).

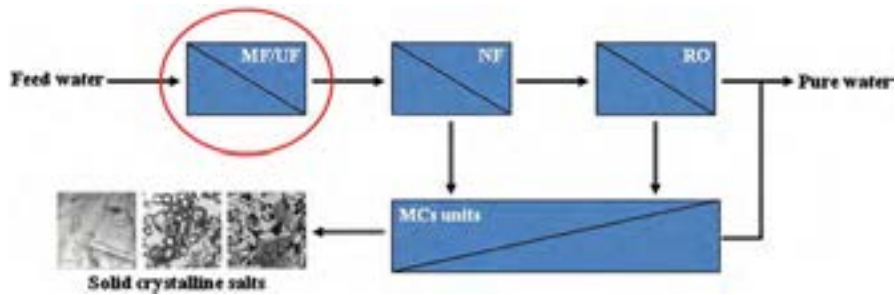


Fig. 1. The flow sheet of an integrated membrane system for seawater desalination (<http://medina.unical.it>).

membrane fouling, which leads to the increase of the hydraulic resistance, the reduction of recovery factor and flux, thus increasing operational costs. On the other side, in submerged UF (sUF), a cross-flow stream over the membrane surface is produced by air bubbling which induces a moderate shear stress generating the back transport of deposited matter [27]; this will have a great significance for reducing particles deposition on the membrane surface and for prolonging the operation period [28]. Furthermore, the sUF technology is worthy of consideration because of the lower energetic consumption and cleaning requirements compared to tangential filtration mode [29,30], while hollow fibers would be preferred over flat sheet membrane configuration due to the higher energy efficiency in terms of creating completely mixed conditions [31] and the increased available membrane surface for module unit volume.

Even though sUF systems have been widely used for the treatment of surface water and wastewater, like in membrane bioreactors, not many attention has been devoted so far to the application of this technology as pretreatment SWRO desalination, and only few papers can be found in the literature [32,33]. However, natural seawater composition in terms of main foulants is quite different from surface water and wastewater. In addition, the higher salt concentration can also affect the interactions existing between membrane-foulant and foulant-foulant, so that a different fouling dynamics is expected to occur. In this situation, the influence on the process of several operating conditions, like the filtration mode, air scouring procedure and backflushing and their effect on membrane fouling needs investigations.

Accordingly, this paper focuses on the study of submerged hollow fibers UF as pretreatment to control natural organic matter content in the seawater to be fed to RO units, in the logic of an integrated membrane desalination system as that shown in Fig. 1, and on the investigation of the influence of a set of operating conditions on process performance and fouling dynamics when working under subcritical flux conditions for relative long operation time.

## 2. Material and methods

Polyethersulfone hollow fiber membranes (from Membrana GmbH, Germany) were used to assemble the one-side potted modules with the total membrane area of 0.068 m<sup>2</sup>. Membrane characteristics are reported in Table 1. Membrane fibers have asymmetric structure with larger pore size on the shell side. Modules were prepared in

Table 1  
Membrane characteristics.

Brand name	UltraPes
Membrane material	Polyethersulfone (PES)
Membrane configuration	Hollow fiber
MWCO	70 ± 20 kDa
Nominal permeability	3.9 L h <sup>-1</sup> m <sup>-2</sup> kPa <sup>-1</sup> @ 23 °C
Wall thickness	150 ± 35 μm
Inner diameter	700 ± 150 μm
Module membrane area	0.068 m <sup>2</sup>

noncarterized configuration to allow more freedom for fibers motion to reduce fouling under air scouring conditions.

Hollow fibers were oriented in vertical arrangement to ensure better performance while bubbling air [34]. Membrane module was used in a bench-scale plant with a maximum working volume of 20 L and operated in submerged configuration as shown in Fig. 2. Filtration was carried out in outside-to-inside mode. Air sparging through a diffuser, at 8 L min<sup>-1</sup> (7.6 m<sup>3</sup> h<sup>-1</sup> m<sup>-2</sup>), was operated from the bottom of the module. The permeate has been drawn by a peristaltic pump towards a permeate tank and then recycled into the module tank. Backflushing have been operated with the permeate. The transmembrane pressure *TMP* (kPa) and flux *J* (L m<sup>-2</sup> h<sup>-1</sup> - LMH) were measured by rotamers and pressure gauges, respectively, and periodically recorded manually. An air line was inserted in the plant to check, when necessary, module integrity.

Seawater from the Tyrrhenian coast (location: Belvedere Marittimo, Calabria, Southern Italy), without any initial pretreatment, was used to feed the plant. Water was uptake 2–3 m far, on the sea side, from the estuarine of a little torrent in which the effluent from a traditional municipal wastewater depuration plant is discharged after treatment. Accordingly, no further source of organic carbon was added to water.

For each operating conditions, a 30 mL sample was withdrawn from the permeate tank and the same amount of feed water was added to the module tank to maintain the feed water level. Water characterization was carried out by ion chromatography (Metrohm IC861 compact system) for ion composition. Content of natural organic matter were evaluated by a TOC analyzer (Shimadzu VCSN) for dissolved organic carbon (DOC), according to standard procedure for seawater, and UV absorbance (UVA) at 254 nm (for the aromatic fraction) and at 210 nm (for amino compounds) by a UV-visible spectrophotometer (UV-1601 Shimadzu), with a 1 cm quartz cell. Samples were filtered by 0.45 μm filters before analysis. Feed water characteristics are provided in Table 2.

Before the experiments, membrane compaction has been carried out by a sequence of increasing and reducing pressure filtration cycles with pure water. After membrane compaction, and before the experimental session, the filtration resistance of the membrane module was determined, through measuring the flux to pure water for increasing trans-membrane pressures steps, by using Darcy's equation:

$$J = \frac{TMP}{\mu R_t} \quad (1)$$

where  $\mu$  (Pa s) is the viscosity of the permeate and  $R_t$  (m<sup>-1</sup>) is the total membrane resistance, coinciding with the intrinsic module resistance  $R_m$  (m<sup>-1</sup>). SW filtration experiments were carried out in either constant trans-membrane pressure or constant flux, while recording the variable parameter *J* or *TMP*, for increasing *TMP* or *J* steps, respectively. The duration of each step was 30 minutes to ensure accuracy and validity of the results. Tests were performed at room temperature around to 24–28 °C.

In order to describe the dynamics and the reversible/irreversible nature of fouling, pressure cycling runs were performed while checking

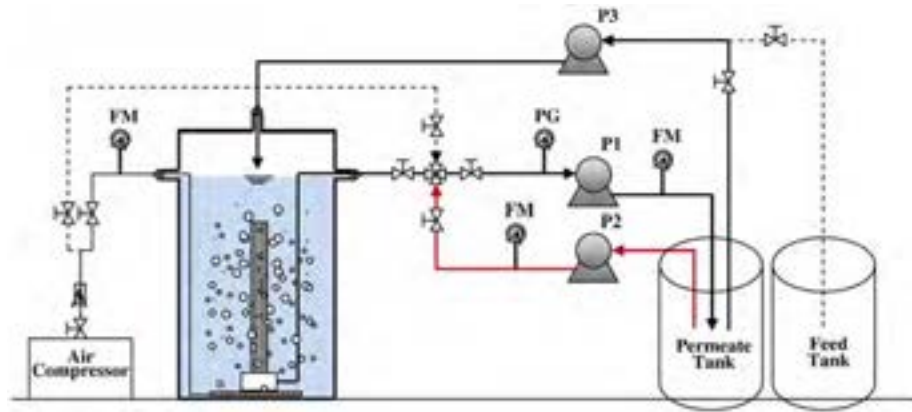


Fig. 2. Laboratory-scale plant used in this work. The permeate is drawn by a peristaltic pump (P1) towards a permeate tank and then recycled into the module tank (P3). Backflushing is operated by a backflushing pump (P2) with the permeate. An air line is used to check module integrity (dotted line). The transmembrane pressure and flux are measured by rotameters (FM) and pressure gauges (PG), respectively. The maximum working volume is 20 L.

flux decrease due to accumulation of foulants on the membrane over continuous filtration. The effect of aeration conditions on fouling rate have been investigated by operating in continuous or periodic aeration/filtration mode. Backflushing with permeate and membrane cleaning with 0.3 wt.% NaOCl solution were performed to recovery permeability. The surface of the membranes was examined by a Quanta 200 F FEI Philips scanning electron microscopy (SEM).

### 3. Results and discussions

#### 3.1. Membrane compaction

Fig. 3 shows the variation of membrane permeability  $L_p$  ( $L h^{-1} m^{-2} kPa^{-1}$ ) to pure water for increasing and decreasing transmembrane pressure cycles. The hysteresis due to membrane compaction is clearly visible for three consecutive cycles. Compaction is a compression of the membrane structure under a  $TMP$  difference causing a decrease in membrane permeability due to mechanical deformation of the solid polymer. Because the hollow fiber have asymmetric structure, the increase of pressure causes densification of the more porous support layer leading to a thickening of the skin layer (selective barrier). Consequently, thicker membranes result in lower permeability and gradual decrease in permeability over the duration of compaction time was observed for each cycle.

In the first cycle, upon increasing  $TMP$  from 5 to 45 kPa,  $L_p$  decreased of almost 50%. At the end of the first relaxation sequence,  $L_p$  at 5 kPa (corresponding to the maximum variation) reduced to the 40% of its initial value at the same  $TMP$ . For  $TMP$  5 kPa,  $L_p$  reduced of 22% and 19% with respect to the initial value for the second and third cycles, respectively. Compaction sequences was considered completed when the maximum variation of  $L_p$  reduced to less than 15% with

respect to the initial value, which occurred after the fifth cycle. At the end of compaction process  $L_p$  stabilized at a value somewhat lower than that indicated by the manufacturer.

#### 3.2. Determination of subcritical flux permeation conditions

To identify the appropriate operating conditions in which fouling can be avoided (or consistently be reduced), the critical flux ( $J_c$ ) has been estimated. The critical flux [35–38] is in fact defined as that flux below which, on start-up, a decline of flux with time does not occur, or is relatively low; when the permeation flux is below  $J_c$  (conditions referred to as subcritical), no particle accumulation occurs in the region of the membrane and filtration can take place in stable conditions close to a permeation operation in clean water.

By plotting  $J$  against  $TMP$  it is possible to observe the transition between constant and nonconstant permeability at the onset of fouling. A common practice to estimate  $J_c$  is to incrementally increase the flux for a fixed duration for each increment, giving a stable  $TMP$  at low flux but an ever-increasing rate of  $TMP$  increase at fluxes beyond  $J_c$  [39–42]. This method is preferred over the  $TMP$ -step method since it provides better control of the flow of material deposition on the membrane surface, as the convective flow of solute towards the membrane is constant during the run [41–43]. Fig. 4 shows the transmembrane flux and pressure as a function of the time for increasing  $J$  operating mode. Experimental points identify two regions. In the first zone, for  $J$  up to around 26 LMH,  $TMP$  increases at a lower rate, although fouling occurred at somewhat extent even for low values (see inset in Fig. 4). For  $J$  greater than 35 LMH,

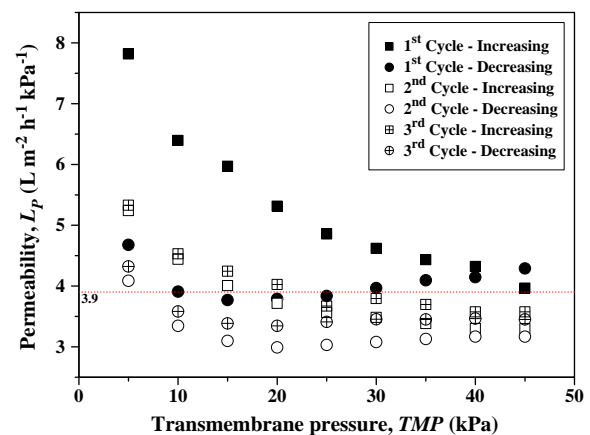


Fig. 3. Membrane compaction before seawater filtration experiments. The dotted line indicates the reference permeability value to pure water provided by the manufacturer.

Table 2  
Composition of feed seawater.

pH	7.9
DOC ( $mg L^{-1}$ )	$1.55 \pm 0.18$
UVA <sub>210</sub> ( $cm^{-1}$ )	$2.25 \pm 0.07$
UVA <sub>254</sub> ( $cm^{-1}$ )	$0.042 \pm 0.004$
SUVA ( $L m^{-1} mg^{-1}$ )	2.71
Conductivity ( $mS cm^{-1}$ )	48.6
Na <sup>+</sup> ( $mg L^{-1}$ )	11731.2
K <sup>+</sup> ( $mg L^{-1}$ )	366.8
Mg <sup>2+</sup> ( $mg L^{-1}$ )	1410.1
Ca <sup>2+</sup> ( $mg L^{-1}$ )	403.7
F <sup>-</sup> ( $mg L^{-1}$ )	1.7
Cl <sup>-</sup> ( $mg L^{-1}$ )	18017.6
Br <sup>-</sup> ( $mg L^{-1}$ )	59.6
SO <sub>4</sub> <sup>2-</sup> ( $mg L^{-1}$ )	2643.0

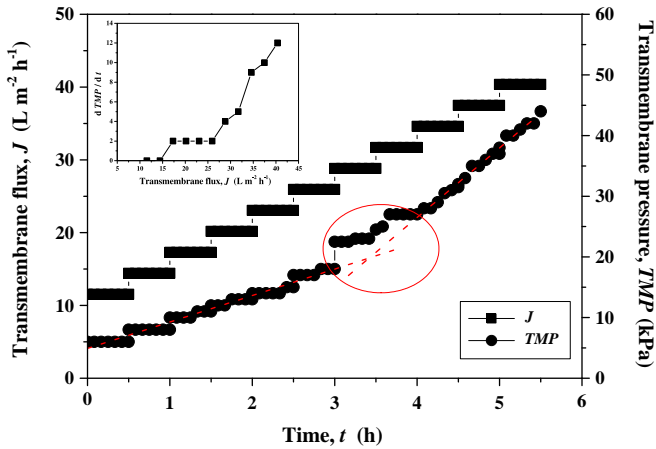


Fig. 4. Transmembrane flux ( $J$ ) and transmembrane pressure ( $TMP$ ) as a function of the time ( $t$ ) for seawater filtration tests, at increasing flux steps. The circle evidences the range of values where fouling started to become more consistent. Red dotted lines are linear fittings to some portions of the  $TMP$  vs. the  $t$  curve. In the inset of the figure the increases of  $TMP$  in the time for increasing flux steps is displayed.

the increase of  $TMP$  was steeper, accounting for a more severe fouling in these permeation conditions. Therefore,  $J_c$  has been considered to lie around to 26 LMH, although increase in  $TMP$  was appreciable already for subcritical permeating conditions.

Two distinct forms of the concept of critical flux have been defined [35]. In the strong form, the flux obtained during subcritical flux is equated to the clean water flux obtained under the same conditions, as adsorption between solute and membrane is negligible, but the  $TMP$ - $J$  curve starts to deviate from that of pure water after  $J_{cs}$  (strong form) has been reached. In the alternative weak form, it is assumed that there is very rapid fouling on start-up and so the  $J$ - $TMP$  relationship is below that of the pure water line. The critical flux (weak form)  $J_{cw}$  is the point at which this line becomes nonlinear.

Fig. 5 shows the  $J$ - $TMP$  relation for constant pressure filtration experiments of pure water and SW in different operating conditions. It is evident that the seawater curves diverge from the pure water since the lower values of  $TMP$ , due to the adsorption of foulants yet at the beginning of the test. According to the definition, this is consistent with a weak-form of critical flux which can be individuated already for low values of  $J$ , indicating that a rather low, but nonzero, rate of membrane fouling is detected even under subcritical flux conditions due to the coupling interactions of components in seawater and

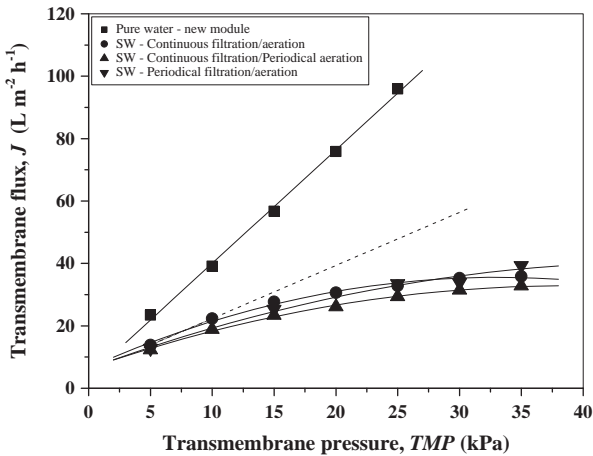


Fig. 5. Transmembrane flux ( $J$ ) as a function of the transmembrane pressure ( $TMP$ ) for pure water and seawater filtration test in continuous and periodical aeration/filtration regimes, at increasing pressure steps. The dotted line is a guide for the eyes.

membrane. From the figure, in accordance with data reported in Fig. 4, the  $J$ - $TMP$  curve starts to be not linear already for  $J = 26$  LMH, this value representing  $J_{cw}$ .

### 3.3. Effect of filtration/aeration operation mode

In order to study the combined effect of aeration/filtration operation mode on process performances, different experimental sections were performed: (i) continuous aeration and filtration, (ii) continuous filtration and periodical aeration (10 min ON/10 min OFF), (iii) periodical filtration (8 min ON/2 min OFF) and aeration (10 min ON/10 min OFF). Fig. 5 compares fluxes against  $TMP$  for SW filtration in these conditions. The curves in the figure demonstrates that the different operation mode only slightly affects fouling dynamics and limiting flux  $J_{cs}$ , as the curves for the three operating conditions display almost the same behavior under the accuracy of the measurement method. Accordingly, system performance in periodical aeration/filtration conditions does not substantially decrease permeate productivity in terms of flux limitations with respect to continuous aeration/filtration mode. On the other side, periodical aeration/filtration operation would be preferred in terms of energy consumption in large scale installations.

To better characterize membrane fouling dynamics in continuous operation, pressure cycling experiments [38,44] have been carried out. Trans-membrane pressure was varied in the time, with cycling steps of 30 minutes, as shown in Fig. 6a.  $TMP$  was increased from subcritical permeation conditions up to 25 kPa, simulating a continuous process. The membrane permeability to SW for each pressure step was obtained

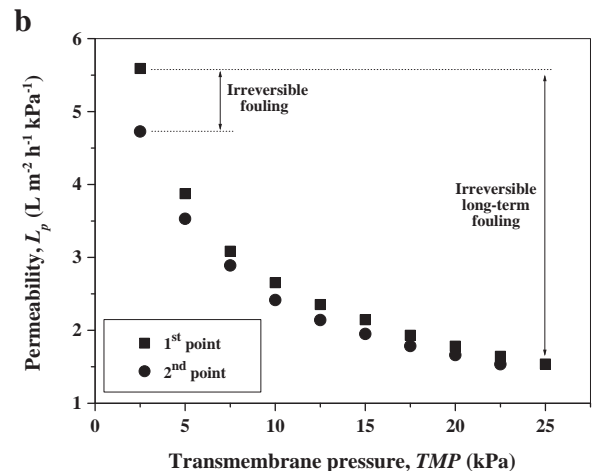
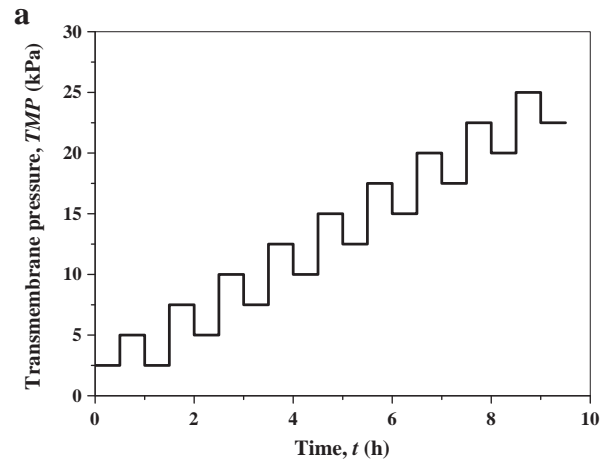


Fig. 6. Cycling pressure experiment (a) and corresponding membrane permeability measurements (b) for seawater filtration experiments.

from the  $J$ - $t$  curves. By this procedure, the evolution of flux limitations and the accumulation of irreversible fouling during continuous operation were estimated.

As shown in Fig. 6b, for low  $TMP$  the main part of fouling was irreversible as  $L_p$  decreased of almost 15% when cycling  $TMP$  in the range 2.5–5–2.5 kPa. Upon increasing  $TMP$  up to 25 kPa, membrane permeability decreased by more than 75% of its original value at 2.5 kPa. For increasing  $TMP$ , the decrease in  $L_p$  was almost entirely reversible, indicating that the irreversible adsorption of foulants occurred yet during the initial stages of the test. This result is consistent with previous considerations and with enhanced probability for a new membrane to be blocked irreversibly [45].

### 3.4. Long term operation conditions

Taking into account previous results, in a subsequent filtration test, plants were run for more than 60 h to simulate continuous operation at the constant subcritical filtration flux of 25 LMH, periodic filtration/aeration and backflushing with the permeate (5 min), while registering  $TMP$  (Fig. 7). The continuous increase of  $TMP$  was observed over the whole operation time, caused by the continuous accumulation of foulants in the region of the membrane. However, two regions can be identified in the graph. In region I, from the start-up to 24 h,  $TMP$  slightly increased from 7 to 15 kPa. In region II,  $TMP$  increased at a higher rate, up to 50 kPa, indicating the enhanced fouling rate in spite of backflushing.

After continuous running, membrane resistance was estimated by using Eq. (1), performing filtration tests with pure water and registering  $J$  at constant  $TMP$ . Fig. 8 shows the variation of the total module resistance  $R_t$  with the cumulative filtered volume of seawater. For  $V=0$  (new module)  $R_m$  was found to be  $2.08 \times 10^{12} \text{ m}^{-1}$ . After almost 120 L of filtered seawater (63 h continuous filtration),  $R_t$  increased up to  $2.54 \times 10^{12} \text{ m}^{-1}$ . At this point, the module was cleaned by soaking in pure water, so that  $R_t$  deceased to  $2.18 \times 10^{12} \text{ m}^{-1}$ . Afterwards, two short SW filtration runs were operated. At this stage, the resistance increased due to further fouling and a sequence of permeate backflushing and soaking in pure water were performed. From the figure it is evident that backflushing with the permeate induced an increase in  $R_t$  while soaking with pure water was effective in recovering, to some extent, membrane permeability. This demonstrated that backflushing induced compaction of the fouling deposits on the membrane while small molecular weight foulants, not rejected by the membrane and existing in the permeate, might break into the pores with the consequent increase of the hydraulic resistance and loss in permeability.

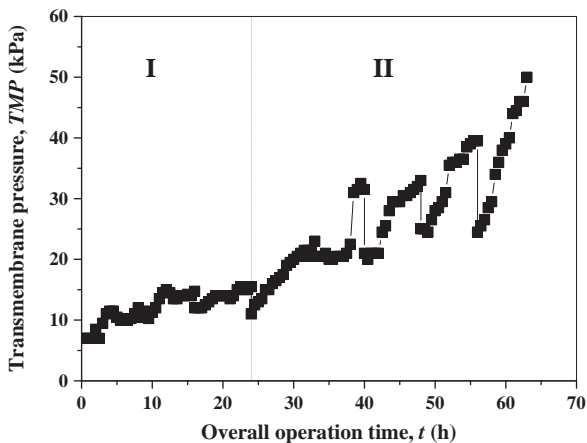


Fig. 7. Variation of the transmembrane pressure  $TMP$  with the cumulative running time  $t$  during long-time operation test.

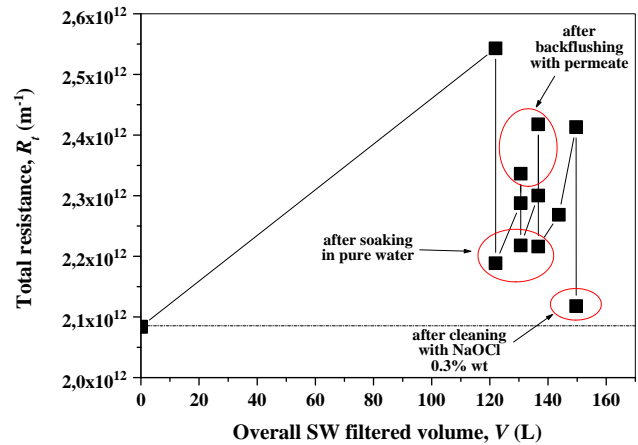


Fig. 8. Total module resistance  $R_t$  as a function of the total amount of SW volume filtered over the effective operating time.

A similar effect has been described previously [46,47]. At the end of the filtration runs  $R_t$  increased up to  $2.41 \times 10^{12} \text{ m}^{-1}$  so that chemical cleaning by NaOCl 0.3% solution was performed. By chemical cleaning, almost complete membrane permeability was recovered, as showed in the last point in Fig. 8.

Fig. 9 shows SEM images of the membrane surface after the SW filtration experiments and after chemical cleaning. Fig. 9a and b illustrates organic particles deposited on both shell and lumen sides of the membrane after SW filtration and before cleaning. As displayed, organic fouling is present even on the lumen side. This is due to the deposit of some NOM existing in the permeate, passed through the membrane during filtration, and compacted on the inner surface during backwashing, thus increasing  $R_t$ . The asymmetric structure of the membrane might help in retaining this organic substance on the inner surface during backflushing because of the smaller pore size. These deposits were efficaciously removed, on both sides, only after chemical cleaning, as demonstrated in Fig. 9c and d.

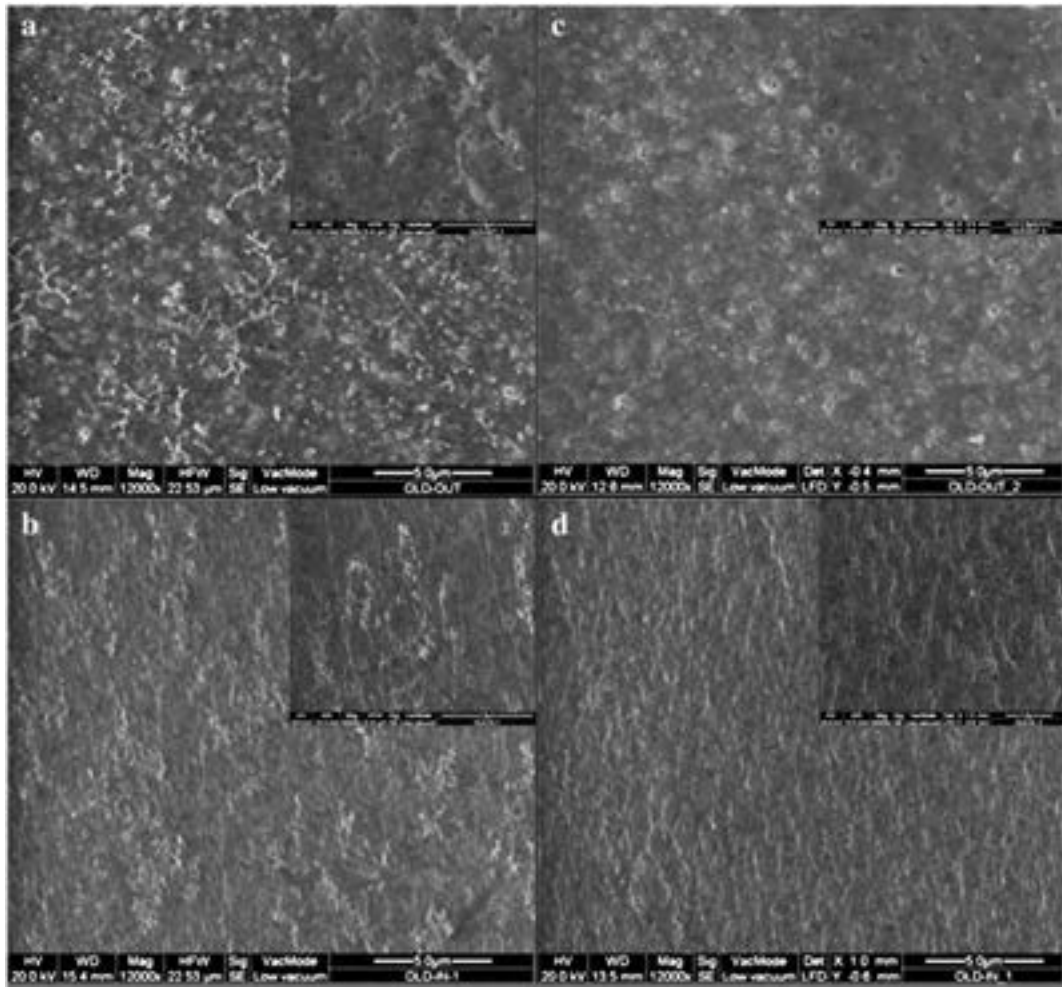
### 3.5. NOM removal from seawater

Fig. 10 displays the rejection of DOC with respect to  $J$  in subcritical flux conditions. The rejection coefficient  $R$  is defined as

$$R = 1 - \frac{C_p}{C_f} \quad (2)$$

where  $C_p$  is the concentration in the permeate and  $C_f$  is the concentration in feed water.

The removal efficiency of DOC displays a slight decreasing trend with  $J$ , spanning from 67% to 24%, with an average of 46%, over the range of  $J$  investigated. DOC content in the permeate resulted always well below  $1 \text{ mg L}^{-1}$  for any value of  $J$  (except for the highest flux). In the figure, the rejection of NOM particles absorbing UV radiation at 254 nm ( $UVA_{254}$ ) and 210 nm ( $UVA_{210}$ ) is also reported.  $UVA_{254}$  provides information on the relative proportions between UV-absorbing unsaturated (aromatic carbon) compounds in NOM. As unsaturated NOM in seawater mainly consists in humic substances [48,49], measurement of  $UVA_{254}$  on the permeate would provide information on humic substances rejection in the process. On the other side, functional (amino) groups absorb UV light more effectively at 210 than at 254 nm. Accordingly, increased absorbance at 210 identifies a greater concentration for amino compounds than for humic substances. Data in Fig. 10 demonstrate that  $UVA_{210}$  is not affected during filtration, as the fraction of NOM absorbing at this wavelength is not



**Fig. 9.** SEM images of membrane fibers: (a) shell side and (b) lumen side at the end of SW filtration; (c) shell side and (d) lumen side after cleaning with NaOCl 0.3% wt. (insets in the figures are images at higher magnification).

effectively removed by SUF. On the other side, the rejection of NOM absorbing UV radiation at 254 nm increases with  $J$ . Organic matter composition in seawater is mainly due to: high molecular weight biopolymers (polysaccharides, proteins), humic substances (mainly fulvic acids), building blocks (hydrolysates of humic substances), low

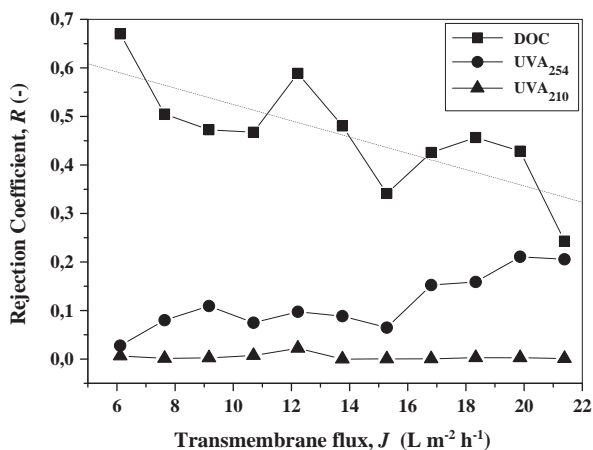


**Fig. 10.** DOC,  $UVA_{254}$  and  $UVA_{210}$  rejection coefficient in seawater filtration test as function of transmembrane flux. The dotted line is a guide for the eyes.

molecular weight acids (organic acids) and low molecular weight neutrals and amphiphilics (mono-oligosaccharides, aminoacids, alcohols, etc.) [50,51]. Results in Fig. 10 demonstrate that organic matter retained by membrane pretreatment consists mainly of high molecular weight biopolymers (not absorbing UV radiation), which are more effectively rejected, and, to some extent, of humic substances, which are only partially retained, while low molecular weight components (absorbing at 210 nm) infiltrate the membrane passing in the permeate. As  $J$  increases, polarization phenomena, which encourage small organic particles to permeate the membrane, increase as well, with the consequent reduction in the overall DOC removal, although the slight increase in the retention of humic substances.

In an integrated membrane system as that described above, NOM would provoke two detrimental effects if not adequately removed by pretreatment: (1) to affect crystallization mechanisms, thus leading to undesirable and irreproducible crystal characteristics, and (2) to induce fouling of both RO and MD/MCr membranes, with the consequent reduction of the overall process efficiency. Curcio et al. [52] demonstrated that the presence of humic acid (HA) ( $2 mg L^{-1}$ ) in solution, kinetically inhibited the nucleation of calcium carbonate crystals, by increasing induction time and reducing initial growth rate by 67%, and consistently affected MD performance, due to the drastic transmembrane flux reduction (up to 45%) with respect to solution without HA. According with the results reported here, submerged hollow fiber UF has been demonstrated as a feasible pretreatment to seawater in reducing DOC well below  $1 mg L^{-1}$ .

#### 4. Conclusions

Experiments performed on direct seawater pretreatment by submerged hollow fiber ultrafiltration demonstrated that:

- Periodical aeration/filtration represents the best compromise between process efficiency and energy consumption, provided the requirements of permeate production.
- The plant can be operated for more than 60 h without any chemical cleaning; however the fouling rate increased yet after 24 h, even when backflushing, with significant loss of performance.
- Irreversible particles adsorption on/in the membrane surface occurs yet during the early stages of seawater filtration, even under subcritical flux conditions.
- Small molecular weight amino compounds permeate the membranes, while biopolymers and, to some extent, humic substances are more effectively retained.
- Excessive backflushing with the permeate, containing not-retained low molecular weight NOM, might not only lead to increased energy consumption and reduced water productivity, but also induces pore blocking and fouling cake compaction on the lumen side of the asymmetric membrane, thus enhancing the overall resistance to mass transport.
- DOC average removal was around to 46%, with a maximum of 67% at lower transmembrane flux, with an average content in the permeate well below  $1 \text{ mg L}^{-1}$ .
- Simple cleaning with NaOCl allows almost complete recovery of original membrane permeability.

According to the results, submerged UF hollow fiber has been demonstrated as a feasible pretreatment to seawater in reducing NOM, thus supporting its utilization as seawater pretreatment in the logic of integrated membrane desalination systems, provided the identification of the operating conditions and their opportune optimization.

#### Acknowledgement

The authors would like to thank the European Commission for the financial support (MEDINA Project: “Membrane-Based Desalination: An Integrated Approach,” Contract Number 036997).

#### References

- [1] J.-C. Charpentier, Modern chemical engineering in the framework of globalization, sustainability, and technical innovation, *Industrial and Engineering Chemistry Research* 46 (2007) 3465–3485.
- [2] T. Van Gerven, A. Stankiewicz, Structure, energy, synergy, times, *The Fundamentals of Process Intensification*, *Industrial and Engineering Chemistry Research* 48 (2009) 2465–2474.
- [3] E. Drioli, A. Criscuoli, E. Curcio, Integrated membrane operations for seawater desalination, *Desalination* 147 (1–3) (2002) 77–81.
- [4] E. Drioli, E. Curcio, A. Criscuoli, G. Di Profio, Integrated system for recovery of  $\text{CaCO}_3$ , NaCl and  $\text{MgSO}_4 \cdot 7\text{H}_2\text{O}$  from nanofiltration retentate, *Journal of Membrane Science* 239 (1) (2004) 27–38.
- [5] X. Ji, E. Curcio, S. Al Obaidani, G. Di Profio, E. Fontananova, E. Drioli, Membrane distillation-crystallization of seawater reverse osmosis brines, *Separation and Purification Technology* 71 (1) (2010) 76–82.
- [6] E. Drioli, E. Curcio, G. Di Profio, F. Macedonio, A. Criscuoli, Integrating membrane contactors technology and pressure-driven membrane operations for seawater desalination: Energy, exergy and costs analysis, *Chemical Engineering Research and Design* 84 (3) (2006) 209–220.
- [7] S.C.J.M. van Hoof, A. Hashim, A.J. Kordes, The effect of ultrafiltration as pretreatment to reverse osmosis in wastewater reuse and seawater desalination applications, *Desalination* 124 (1999) 231–242.
- [8] A. Teuler, K. Glucina, J.M. Lain, Assessment of UF pretreatment prior RO membranes for seawater desalination, *Desalination* 125 (1999) 89–96.
- [9] A. Brehant, V. Bonnelye, M. Perez, Comparison of MF/UF pretreatment with conventional filtration prior to RO membranes for surface seawater desalination, *Desalination* 144 (1–3) (2002) 353–360.
- [10] P. Glueckstern, M. Priel, M. Wilf, Field evaluation of capillary UF technology as a pretreatment for large seawater RO systems, *Desalination* 147 (2002) 55–62.
- [11] C.K. Teng, M.N.A. Hawlader, A. Malek, An experiment with different pretreatment methods, *Desalination* 156 (1–3) (2003) 51–58.
- [12] G.K. Pearce, S. Talo, K. Chida, A. Basha, A. Gulamhusein, Pretreatment options for large scale SWRO plants: Case studies of UF trials at Kindasa, Saudi Arabia, and conventional pretreatment in Spain, *Desalination* 167 (2004) 175–189.
- [13] P.H. Wolf, S. Siverns, S. Monti, UF membranes for RO desalination pre-treatment, *Desalination* 182 (2005) 293–300.
- [14] D. Gille, W. Czolkoss, Ultrafiltration with multi-bore membranes as seawater pre-treatment, *Desalination* 182 (2005) 301–307.
- [15] M. Kumar, S.S. Adham, W.R. Pearce, Investigation of seawater reverse osmosis fouling and its relationship to pretreatment type, *Environmental Science and Technology* 40 (6) (2006) 2037.
- [16] W. Ma, Y. Zhao, L. Wang, The pretreatment with enhanced coagulation and a UF membrane for seawater desalination with reverse osmosis, *Desalination* 203 (1–3) (2007) 256–259.
- [17] O. Lorain, B. Hersant, F. Persin, A. Grasmick, N. Brunard, J.M. Espenan, Ultrafiltration membrane pre-treatment benefits for reverse osmosis process in seawater desalting. Quantification in terms of capital investment cost and operating cost reduction, *Desalination* 203 (1–3) (2007) 277–285.
- [18] G.K. Pearce, The case for UF/MF pretreatment to RO in seawater applications, *Desalination* 203 (2007) 286–295.
- [19] J. Xu, G.L. Ruan, X.Z. Chu, Y. Yao, B.W. Su, C.J. Gao, A pilot study of UF pretreatment without any chemicals for SWRO desalination in China, *Desalination* 207 (2007) 216–226.
- [20] J. Xu, G.L. Ruan, X.L. Gao, X.H. Pan, B.W. Su, C.J. Gao, Pilot study of inside-out and outside-in hollow fiber UF modules as direct pretreatment of seawater at low temperature for reverse osmosis, *Desalination* 219 (1–3) (2008) 179–189.
- [21] N. Prihasto, Q.-F. Liu, S.-H. Kim, Pre-treatment strategies for seawater desalination by reverse osmosis system, *Desalination* 249 (2009) 308–316.
- [22] F. Knops, R. te Lintelo, Long-term operating experience of Seaguard UF as pretreatment to SWRO in the Mediterranean region, *Desalination and Water Treatment* 5 (2009) 74–79.
- [23] V. García-Molina, R. Chang, M. Busch, First year performance review of Magong UF/RO seawater desalination plant, *Desalination and Water Treatment* 13 (2010) 203–212.
- [24] N. Voutchkov, Considerations for selection of seawater filtration pretreatment system, *Desalination* 261 (2010) 354–364.
- [25] D.F. Halpern, J. McArdle, B. Antrim, UF pretreatment for SWRO: Pilot studies, *Desalination* 182 (2005) 323–332.
- [26] M. Wilf, M.K. Schierach, Improved performance and cost reduction of RO seawater systems using UF pretreatment, *Desalination* 135 (2001) 61–68.
- [27] Z.F. Cui, S. Chang, A.G. Fane, The use of gas bubbling to enhance membrane processes, *Journal of Membrane Science* 221 (2003) 1–35.
- [28] J. Tian, Y.-P. Xu, Z.-L. Chen, J. Nan, G.-B. Li, Air bubbling for alleviating membrane fouling of immersed hollow-fiber membrane for ultrafiltration of river water, *Desalination* 260 (1–3) (2010) 225–230.
- [29] M. Gander, B. Jefferson, S. Judd, Aerobic MBRs for domestic wastewater treatment: A review with cost considerations, *Separation and Purification Technology* 18 (2000) 119–130.
- [30] A.G. Fane, A. Yeo, A. Law, K. Parameshwaran, F. Wicaksana, V. Chen, Low pressure membrane processes doing more with less energy, *Desalination* 185 (2005) 159–165.
- [31] Y. Wang, M. Brannock, G. Leslie, Membrane bioreactors: Overview of the effects of module geometry on mixing energy, *Asia-Pacific Journal of Chemical Engineering* 4 (2009) 322–333.
- [32] P. Côté, J. Cadera, J. Coburn, A. Munro, A new immersed membrane for pretreatment to reverse osmosis, *Desalination* 139 (1–3) (2001) 229–236.
- [33] J.-B. Castaing, A. Massé, M. Pontié, V. Séchet, J. Haure, P. Jaouen, Investigating submerged ultrafiltration (UF) and microfiltration (MF) membranes for seawater pre-treatment dedicated to total removal of undesirable micro-algae, *Desalination* 253 (1–3) (2010) 71–77.
- [34] A.G. Fane, S. Chang, E. Chardon, Submerged hollow fibre membrane module: Design options and operational considerations, *Desalination* 146 (2002) 231–236.
- [35] R.W. Field, D. Wu, J.A. Howell, B.B. Gupta, Critical flux concept for microfiltration fouling, *Journal of Membrane Science* 100 (3) (1995) 259–272.
- [36] P. Bacchin, P. Aimar, V. Sanchez, Model for colloidal fouling of membranes, *AIChE Journal* 41 (2) (1995) 368–377.
- [37] J.A. Howell, Sub-critical flux operation of microfiltration, *Journal of Membrane Science* 107 (1–2) (1995) 165–171.
- [38] P. Bacchin, P. Aimar, R.W. Field, Critical and sustainable fluxes: Theory, experiments and applications, *Journal of Membrane Science* 281 (1–2) (2006) 42–69.
- [39] V. Chen, A.G. Fane, S.S. Madaeni, I.G. Wenten, Particle deposition during membrane filtration of colloids: Transition between concentration polarization and cake formation, *Journal of Membrane Science* 125 (1) (1997) 109–122.
- [40] E.H. Bouhabila, R. Ben Aim, H. Buisson, Microfiltration of activated sludge using submerged membrane with air bubbling (application to wastewater treatment), *Desalination* 118 (1–3) (1998) 315–322.
- [41] L. Defrance, M.Y. Jaffrin, Comparison between filtrations at fixed transmembrane pressure and fixed permeate flux: Application to a membrane bioreactor used for wastewater treatment, *Journal of Membrane Science* 152 (2) (1999) 203–210.
- [42] L. Defrance, M.Y. Jaffrin, Reversibility of fouling formed in activated sludge filtration, *Journal of Membrane Science* 157 (1) (1999) 73–84.
- [43] P. Le Clech, B. Jefferson, I.S. Chang, S.J. Judd, Critical flux determination by the flux-step method in a submerged membrane bioreactor, *Journal of Membrane Science* 227 (1–2) (2003) 81–93.

- [44] B. Espinasse, P. Bacchin, P. Aimar, On an experimental method to measure critical flux in ultrafiltration, *Desalination* 146 (1–3) (2002) 91–96.
- [45] K.J. Howe, A. Marwah, K.-P. Chiu, S.S. Adham, Effect of membrane configuration on bench-scale MF and UF fouling experiments, *Water Research* 41 (2007) 3842–3849.
- [46] U. Metzger, P. Le-Clech, R.M. Stuetz, F.H. Frimmel, V. Chen, Characterisation of polymeric fouling in membrane bioreactors and the effect of different filtration modes, *Journal of Membrane Science* 301 (2007) 180–189.
- [47] J. Wu, P. Le-Clech, R.M. Stuetz, A.G. Fane, V. Chen, Effects of relaxation and backwashing conditions on fouling in membrane bioreactor, *Journal of Membrane Science* 324 (2008) 26–32.
- [48] N. Her, G. Amy, H. Park, M. Song, Characterizing algogenic organic matter (AOM) and evaluating associated NF membrane fouling, *Water Research* 38 (6) (2004) 1427–1438.
- [49] N. Park, B. Kwon, S. Kim, J. Cho, Characterizations of the colloidal and microbial organic matters with respect to membrane foulants, *Journal of Membrane Science* 275 (1–2) (2006) 29–36.
- [50] S.A. Huber, Evidence for membrane fouling by specific TOC constituents, *Desalination* 119 (1998) 229–234.
- [51] H.K. Shon, S. Vigneswaran, J. Cho, Comparison of physico-chemical pretreatment methods to seawater reverse osmosis: Detailed analyses of molecular weight distribution of organic matter in initial stage, *Journal of Membrane Science* 320 (2008) 151–158.
- [52] E. Curcio, X. Ji, G. Di Profio, S. Al Obaidani, E. Fontananova, E. Drioli, Membrane distillation operated at high seawater concentration factors: Role of the membrane on CaCO<sub>3</sub> scaling in presence of humic acid, *Journal of Membrane Science* 346 (2) (2010) 263–269.